Journal of Sound and Vibration (1997) **199**(2), 223–236

VIBRATION AND VARIABLE STRUCTURE CONTROL WITH INTEGRAL COMPENSATION IN A NON-CONSTANT ROTATING DISK SYSTEM

R.-F. FUNG

Department of Mechanical Engineering, Chung Yuan Christian University, Chung-Li, Taiwan 32023, *Republic of China*

(*Received* 8 *August* 1995, *and in final form* 26 *March* 1996)

Transverse vibration control is an important task in the application of a rotating disk. Here, a novel control solution based on variable structure control with integral compensation (IVSC) principle is formulated, designed and tested, for the control of the transverse vibration of the disk rotating with non-constant angular velocity. The most distinguishing feature of IVSC is its ability to produce very robust control. In many cases, it is insensitive to parametric uncertainty and improves transient response and steady-state error. In this paper, Hamilton's principle is applied to derive the governing equation for the transverse vibration of the disk rotating with non-constant angular velocity. Galerkin's method is employed to discretize the system into infinite modal equations. The approach is based on the independent modal space control (IMSC), and the IVSC is used to design the control procedure to suppress the transverse vibration of the rotating disk in the cases of constant and non-constant speeds.

1. INTRODUCTION

Centrally clamped rotating disks are the basic machine element of steam and gas turbines, grinding wheels, circular saws, and computer disk memories. Large amplitude transverse vibration of a rotating disk can cause failure of turbine wheels due to wheel-to-case contact, cutting inaccuracy for grinding wheels and circular saws and head tracking errors in computer disk memories. As early as 1921, Lamb and Southwell [1] investigated the transverse vibration of a spinning disk. The vibration of a centrally clamped spinning disk is investigated by Barasch and Chen [2], and Bulkeley [3]. To the author's knowledge, there is no literature study of spinning disks with non-constant angular velocity.

Transverse vibration control is an important task in the application of a rotating disk. Ellis and Mote [4] developed a control system which generated a transverse force in response to the measured transverse displacement and velocity of the disk. This system controlled low frequency vibration, but excited higher frequency instability above the bandwidth of the control system. Radcliffe and Mote [5] used an on-line FET analysis of the dominant mode of the disk response, and designed a spectral controller to suppress it. Auburn and Ratner [6] adopted large space structure control for a circular plate. Kuo and Huang [7] proposed linear compensators whose design was based on a root locus argument to control the vibrations. The control of a disk rotating with non-constant angular velocity was not discussed in the above papers, and some of them neglected membrane stress effects in transverse vibration. In this paper, a novel control solution based on the variable structure system (VSS) principle is formulated, designed and tested,

0022–460X/97/020223 + 14 $25.00/0/sv960611

for the control of the transverse vibration of the disk rotating with non-constant angular velocity. Membrane stress effects are also considered.

Guaranteeing stability of distributed parameter control systems is inherently more difficult than for lumped parameter control systems. When controlling a finite number of modes in a distributed structure, the central stability problem is to isolate the modes of the control system that are not under control. This isolation is accomplished through elimination of either "observation spillover" or "control spillover". In this paper, the approach is based on independent modal space control (IMSC) [8]. That is, the modeled modes are controlled separately. As a result, no spillover or energy transfers from one mode to the others occur. For the purpose of reducing observation spillover, modal filters [9] are employed to synthesize the sensors' output and generate the control forces of actuators. Then, no observation spillover exists.

Variable structure control (VSC) was first proposed and elaborated in the early 1950's in the Soviet Union [10] and [11]. A rise in interest in VSC occurred in the 1970's because its robustness and invariance had been gradually recognized. Since 1980, a general VSC design method had been developed and the property of perfect robustness of a VSC system with rspect to system perturbation and disturbances was fully recognized [12]. Recently, VSC has attracted interest because both fast calculation and switching action have been realized through the progress of micro and power electronics. The dominant role in VSS theory is played by a sliding mode, and the core idea of designing a VSS control algorithm consists of enforcing this type of motion in some of the manifolds in the system state space. The most distinguished feature of VSC is its ability to result in very robust control. In many cases, it is insensitive to parametric uncertainty and external disturbance.

In this paper, Hamilton's principle is applied to derive the governing equation of the disk rotating with non-constant angular velocity. In the distributed system, Galerkin's method is employed to discretize it into infinite modal equations. In the present work, the VSC scheme as proposed by Fung *et al*. [13] is extended to include integral compensation. Due to the powerful prominent characteristic of IVSC, it is convenient to design the control procedure to suppress the transverse vibration of the rotating disk.

2. EQUATION OF MOTION

The analytical model of a rotating flexible disk which is clamped at $r = a$, free at $r = b$, and spinning with a non-constant angular velocity (Figure 1) is considered. The differential equation governing the transverse displacement will be derived by adopting classical plate

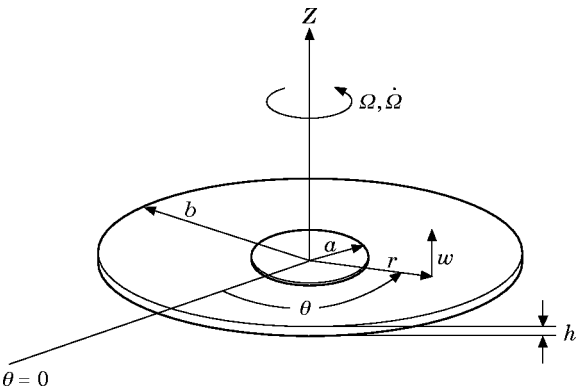

Figure 1. Schematic of the spinning flexible disk system.

theory, and neglecting the effects of rotary inertia as advocated by Benson and Bogy [14] (please see the Appendix for the definitions of the symbols used). For this rotating circular plate, the strain energy is given by

$$U = \frac{D}{2}\int\int\left[\left(w_{rr} + \frac{1}{r}w_r + \frac{1}{r^2}w_\theta\right)^2 - 2(1-v)w_{rr}\left(\frac{1}{r}w_r + \frac{1}{r^2}w_{\theta\theta}\right)\right.$$

$$\left. + 2(1-v)\left(\frac{1}{r}w_{r\theta} - \frac{1}{r^2}w_\theta\right)^2\right] r\,\mathrm{d}r\,\mathrm{d}\theta. \tag{1}$$

Neglecting effects of rotary inertial, the kinetic energy of the rotating disk is

$$T = \frac{1}{2}\int\int \rho h(\Omega^2 w_\theta + 2\Omega w_\theta w_t + w_t^2) r\,\mathrm{d}r\,\mathrm{d}\theta. \tag{2}$$

The potential energy due to stresses caused by centrifugal force can be written as

$$V = \frac{1}{2}\int\int h\left(\sigma_r w_r^2 + \sigma_\theta\left(\frac{1}{r}w_\theta\right)^2\right) r\,\mathrm{d}r\,\mathrm{d}\theta, \tag{3}$$

where σ_r and σ_θ are, respectively, the radial and circumferential stresses in the disk caused by the centrifugal force. They are given by Timoshenko and Goodier [15] as

$$\sigma_r = \Omega^2(C_1 + C_2/r^2 + C_3 r^2), \qquad \sigma_\theta = \Omega^2(C_1 + C_2/r^2 + C_4 r^2),$$

$$C_1 = \frac{1+v}{8}\rho\,\frac{(v-1)a^4 - (3+v)b^4}{(v-1)a^2 - (1+v)b^2}, \qquad C_2 = \frac{1-v}{8}\rho a^2 b^2\,\frac{(v+1)a^2 - (3+v)b^2}{(v-1)a^2 - (1+v)b^2},$$

$$C_3 = -((3+v)/8)\rho, \qquad C_4 = -((1+3v)/8)\rho.$$

It should be noted that $\Omega = \Omega(t)$ for the case of non-constant angular velocity. Hamilton's principle requires that

$$\int_{t_1}^{t_2}(\delta T - \delta U - \delta V)\,\mathrm{d}t = \int_{t_1}^{t_2}\delta\left(\int\int f w\,\mathrm{d}r\,\mathrm{d}\theta\right)\mathrm{d}t, \tag{4}$$

where f is the external load in the transverse direction. Carrying out the first variation and integrating by parts with respect to time and spatial co-ordinates, one obtains the governing equation and boundary condition, respectively, as

$$\rho h(w_{tt} + 2\Omega w_{t\theta} + \Omega^2 w_{\theta\theta} + \dot{\Omega} w_\theta) + D\nabla^4 w - (h/r)(\sigma_r r w_r)_r - (h/r^2)\sigma_\theta w_{\theta\theta} = f, \tag{5}$$

$$(w)_{r=a} = 0, \qquad (w_r)_{r=a} = 0, \qquad [\nabla^2 w - (1-v)(1/r)w_r + (1/r^2)w_{\theta\theta})]_{r=b} = 0, \tag{6a–c}$$

$$\left[\frac{\partial}{\partial r}\nabla^2 w + (1 - v/r)(\partial^2/\partial\theta^2)(w_r - (1/r)w)\right]_{r=b} = 0. \tag{6d}$$

If $\dot{\Omega} = 0$, then the equation is the same as in [4]. Here, the non-dimensional parameters are introduced

$$R = r/b, \qquad W = w/b, \qquad \tau = t\sqrt{D/\rho\pi hb^4},$$

$$\nabla^2 = \partial^2/\partial R^r + \partial/R\partial R + \partial^2/R^2\partial R^2, \qquad \omega = \Omega/\sqrt{D/\rho\pi hb^4}.$$

If the external load is not considered, the following equation can be expressed in non-dimensional form by

$$W_{\tau\tau} + 2\omega W_{\tau\theta} + \omega^2 W_{\theta\theta} + \dot{\omega} w_\theta + D\nabla^4 W - (\omega/b)(C_r W_R + C_{rr} W_{RR} + C_{\theta\theta} W_{\theta\theta}) = 0, \quad (7)$$

where

$$C_r = C_1/bR - C_2/b^3R^3 + 3bRC_3, \qquad C_{rr} = C_1 + C_2/b^2R^2 + b^2R^2C_3,$$

$$C_{\theta\theta} = C_1/bR - C_2/b^3R^3 + bRC_3.$$

3. GALERKIN'S METHOD

The solution of the governing equation is approximated by a Fourier eigenfunction expansion. Using the eigenfunctions of the related problem

$$\nabla^4 W = \lambda^4 W, \quad (8)$$

with the boundary conditions (6a–d), one obtains the eigenvalues λ_{mn} associated with the eigenfunctions

$$\Phi_{mn} = \Theta(m\theta) R_m(\lambda_{mn} R), \quad (9)$$

where

$$\Theta(m\theta) = \begin{Bmatrix} \sin m\theta \\ \cos m\theta \end{Bmatrix},$$

$$R_m(\lambda_{mn}R) = [e_{1m}\mathrm{J}_m(\lambda_{mn}R) + e_{2m}\mathrm{Y}_m(\lambda_{mn}R) + e_{3m}\mathrm{I}_m(\lambda_{mn}R) + e_{4m}\mathrm{K}_m(\lambda_{mn}R)],$$

and J_m, Y_m, I_m and K_m are mth order Bessel function and modified Bessel functions, e_{1m}, e_{2m}, e_{3m}, e_{4m} are constants which can be determined by the normalization condition

$$1 = \pi \int R_m(\lambda_{mn}R) R \, \mathrm{d}R.$$

The vibration modes are described by the number of the nodal circle n and the nodal diameter m. Therefore, the transverse displacement can be described by a modal expansion as

$$W(R, \theta, t) = \sum_{m,n=0}^{\infty} [A_{mn}(\tau)\sin m\theta + B_{mn}(\tau)\cos m\theta] R_m(\lambda_{mn}R). \quad (10)$$

Applying Galerkin's method, substituting (10) into (7), multiplying the resulting equation by $R_m(\lambda_{mn}R)\sin m\theta$ and integrating over the area of the disk and repeating the process with

$R_m(\lambda_{mn}R)\cos m\theta$, one obtains for $m, n \in [0, \infty)$, respectively, the equation of the generalized co-ordinates $A_{mn}(\tau)$, $B_{mn}(\tau)$ as

$$\ddot{A}_{mn} - 2m\omega\dot{B}_{mn} + (\pi\lambda_{mn}^4 - m^2\omega^2 + \pi\omega^2\Pi_m)A_{mn} - m\dot{\omega}B_{mn} = 0, \tag{11a}$$

$$\ddot{B}_{mn} + 2m\omega\dot{A}_{mn} + (\pi\lambda_{mn}^4 - m^2\omega^2 + \pi\omega^2\Pi_m)B_{mn} + m\dot{\omega}A_{mn} = 0, \tag{11b}$$

where

$$\Pi_m = \int \frac{-1}{b} [C_r R_m'(\lambda_{mn}R) + C_{rr}R_m''(\lambda_{mn}R) + C_{\theta\theta}R_m(\lambda_{mn}R)]R_m(\lambda_{mn}R)\,\mathrm{d}R.$$

Equations (11) can be transformed to the state equation

$$\dot{\mathbf{X}} = \mathbf{\Phi}\mathbf{X}, \tag{12}$$

where

$$\mathbf{X} = [\dot{A}_{mn}\ \dot{B}_{mn}\ A_{mn}\ B_{mn}]^{\mathrm{T}}, \quad \mathbf{\Phi} = \begin{bmatrix} \mathbf{G} & \mathbf{K} \\ \mathbf{I} & \mathbf{O} \end{bmatrix},$$

and

$$\mathbf{G} = \begin{bmatrix} 0 & -2m\omega \\ 2m\omega & 0 \end{bmatrix}, \qquad \mathbf{I} = \begin{bmatrix} 1 & 0 \\ 0 & 1 \end{bmatrix}, \qquad \mathbf{O} = \begin{bmatrix} 0 & 0 \\ 0 & 0 \end{bmatrix},$$

$$\mathbf{K} = \begin{bmatrix} -(\pi\lambda_{mn}^4 - m^2\omega^2 + \pi\Pi_m) & -m\dot{\omega} \\ m\dot{\omega} & -(\pi\lambda_{mn}^4 - m^2\omega^2 + \pi\Pi_m) \end{bmatrix},$$

G represents the skew symmetric gyroscopic matrix, which arises from the gyroscopic term $2\omega W_{\tau\theta}$ in (7). Due to the rotation, one finds that the gyroscopic effect takes place in the tangential direction only, and so the coefficients $A_{mn}(\tau)$ and $B_{mn}(\tau)$ of $\sin m\theta$ and $\cos m\theta$ in (10) are coupled and each mode is decoupled from the others.

4. MODIFIED VARIABLE STRUCTURE CONTROL

The schematic of the variable structure with integral compensation (IVSC), the locations of actuators and sensors and block diagram are shown in Figs. (2a–c). The control procedure is described as follows: (i) As in the initial state, the control law is governed by IVSC [16] to get fast response, (ii) once the error reaches zero the control law is switched to the VSC scheme to achieve robust stability.

Let the control input function be in the form

$$U = (1 - E_{q1})U_{VSC} + E_{q1}U_{IVSC}, \tag{13}$$

where U is the control input function, E_{q1} is the selector to choose which controller to be executed, U_{VSC} is the control input of VSC scheme and U_{IVSC} that of the IVSC scheme.

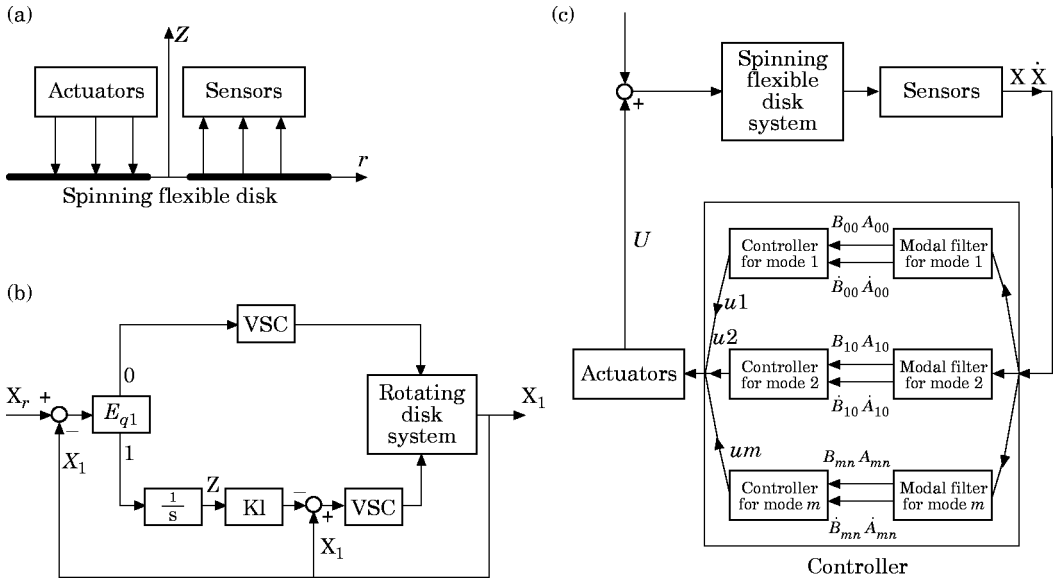

Figure 2. Schematic diagram of the control implementation. (a) Location of actuators and sensors. (b) Modified variable structure control with integral compensation. (c) Block diagram.

4.1. DESIGN OF VSC

The structure in a VSC system is governed by the sign of vector-valued function $S(x)$ that is defined as the switching function. A switching function is generally assumed to be m-dimensional, i.e.,

$$\mathbf{S}(\mathbf{X}) = \mathbf{C}\mathbf{X}, \tag{14}$$

where

$$\mathbf{S}(\mathbf{X}) = [s_1(\mathbf{X}), s_2(\mathbf{X}), \ldots, \mathrm{s_m}(\mathbf{X})]^{\mathrm{T}},$$

$$\mathbf{C} = [\mathbf{c}_1^T, \mathbf{c}_2^T, \ldots, \mathbf{c}_m^T].$$

Each scalar switch function $s_i(\mathbf{X}) = \mathbf{c}_i^T\mathbf{X}$ describes a linear surface $s_i(\mathbf{X}) = 0$, which is defined to be a switching surface function. If, for any initial time t_0, $X(t)$ in S for all $t > t_0$ then $X(t)$ is a sliding motion or the sliding mode of the system. If every point in S is an end point, that is, for every point in S there are trajectories reaching it from both sides of S, S is called a sliding surface.

The present system is modeled by the dynamic equation

$$\dot{\mathbf{X}} = \Phi\mathbf{X} + \Gamma U, \tag{15}$$

where $\mathbf{X} \in R^{m \times 1}$, and Φ, Γ are of appropriate dimensions. Both are introduced in (12) and U is the control input. The design of VSC involves, first, the design of an appropriate m-dimensional switching function $\mathbf{S}(x)$ for the desired sliding mode dynamics, and second, the design of a control for the reaching mode so that such a reaching condition is met.

From the partitions

$$\mathbf{X} = \begin{bmatrix} \mathbf{X}_1 \\ \mathbf{X}_2 \end{bmatrix}, \quad \mathbf{C} = [\mathbf{C}_1 \quad \mathbf{C}_2], \qquad \Phi = \begin{bmatrix} \Phi_{11} & \Phi_{12} \\ \Phi_{21} & \Phi_{22} \end{bmatrix}, \quad \Gamma = \begin{bmatrix} \mathbf{0} \\ \Gamma_2 \end{bmatrix},$$

where the dimension of $\mathbf{X}_1$ is $n \times m$, and using the transformation

$$\begin{bmatrix} \mathbf{X}_1 \\ \mathbf{S} \end{bmatrix} = \begin{bmatrix} \mathbf{I} & \mathbf{0} \\ \mathbf{C}_1 & \mathbf{C}_2 \end{bmatrix} \begin{bmatrix} \mathbf{X}_1 \\ \mathbf{X}_2 \end{bmatrix}, \tag{16}$$

the dynamic equation is transformed to

$$\dot{\mathbf{X}}_1 = (\Phi_{11} - \Phi_{12}C_2^{-1}C_1)\mathbf{X}_1 + \Phi_{12}C_2^{-1}\mathbf{S},$$

$$\dot{S} = [(C_1\Phi_{11} - C_2\Phi_{12}) - (C_1\Phi_{12} + C_2\Phi_{22})C_2^{-1}C_1]\mathbf{X}_1 + (C_1\Phi_{12} + C_2\Phi_{22})C_2^{-1}S + C_2\Gamma_2 U.$$

On the switching manifold $\mathbf{S} = 0$, the differential equation

$$\dot{\mathbf{X}}_1 = (\Phi_{11} - \Phi_{12}C_2^{-1}C_1)X_1, \tag{17}$$

describes the sliding mode of the system (12). If the system is controllable, then it is easy to show that (Φ_{11}, Φ_{12}) are a controllable pair. Thus by a proper choice of the matrix $C_2^{-1}C_1$, poles of the sliding mode can be placed as desired which will then ensure the asymptotic stability and desired responses for the sliding mode.

The condition under which the state will move towards and reach a sliding surface is called a reaching condition. In VSS, the states are forced to slide along the sliding surface. To achieve the sliding regime, proper switching functions ensuring the desired response for the sliding mode are necessary. In the following section, the reaching law method [12] is adopted to design the reaching mode, which satisfies the reaching condition.

4.1.1. *Reaching mode design*

The main requirement in the reaching mode design is that the control should satisfy the reaching condition, which in turn guarantees the existence of the sliding mode on the switching manifold. Additional requirements include fast reaching and no chattering. Specifying a scheme for the switching order is also a part of the VSC design. In the discussion, the reaching law method is introduced.

The reaching law is a differential equation which specifies the dynamics of a switching function. The differential equation of an asymptotically stable switching function is itself a reaching condition. In addition, by the choice of the parameters in the differential equation, the dynamic quality of VSS in the reaching mode can be controlled. Power rate reaching will be introduced in the following form

$$\dot{\mathbf{S}} = \mathbf{Q}\,\mathrm{sgn}(s_i), \tag{18}$$

where

$$\mathbf{Q} = \mathrm{diag}[-P_1|s_1|^\alpha, -P_2|s_2|^\alpha, \ldots, -P_m|s_m|^\alpha], \qquad 0 < \alpha < 1.$$

The reaching law increases the reaching speed when the state is far away from the switching manifold, but reduces the rate when the state is near the manifold. The result is a fast reaching and low chattering reaching mode. It also shows that the reaching time is finite. Integrating (18) from $s_i = s_{i0}$ to $s_i + = 0$ yields

$$t_i = (1/(1-\alpha)p_i)(s_{i0})^{1-\alpha}. \tag{19}$$

4.1.2. *Control law design*

The system is modeled as

$$\dot{\mathbf{X}} = \Phi(\mathbf{X}) + \Gamma U. \tag{20}$$

The control law can be determined now. Computing the time derivative of $\mathbf{S}(\mathbf{X})$ along the reaching mode trajectory and using (17), one obtains

$$\mathbf{C}\Phi(\mathbf{X}) + \mathbf{C}\Gamma U_{VSC} = -\mathbf{Q}\ \mathrm{sgn}\ (s). \tag{21}$$

Noting that the matrix $(\mathbf{C}\Gamma)^{-1}$ is non-singular. Equation (14) can be solved to yield the control law

$$U_{VSC} = -(\mathbf{C}\Gamma)^{-1}[\mathbf{C}\Phi(\mathbf{X}) + \mathbf{Q}\ \mathrm{sgn}\ (s)]. \tag{22}$$

4.2. DESIGN OF IVSC

In this section the approach developed by Chern and Wu [16] is adopted, and the reaching law used to design the IVSC scheme. The switching function is described as:

$$\mathbf{S}(\mathbf{X}) = \mathbf{C}_1(\mathbf{X}_1 - K_I\mathbf{Z}) + \mathbf{C}_2\mathbf{X}_2, \tag{23}$$

where

$$\mathbf{Z} = [z_1, z_2, \ldots, z_m]$$

in which z_i is the integral value of error.

The system is modeled as

$$\dot{\mathbf{Z}} = r - \mathbf{X}_1, \qquad \dot{\mathbf{X}} = \Phi(\mathbf{X}) + \Gamma U_{IVSC}. \tag{24}$$

where r is the reference input. By the reaching law method, $\dot{\mathbf{S}} = -\mathbf{Q}\ \mathrm{sgn}\ (s_i)$, the IVSC control input function can be stated as

$$U_{IVSC} = -(\mathbf{C}\Gamma)^{-1}[\mathbf{C}\Phi(\mathbf{X}) + \mathbf{Q}\ \mathrm{sgn}\ (s) - \mathbf{C}_1K_I(r - \mathbf{X}_1)]. \tag{25}$$

5. MODAL SPACE CONTROL

Control of an infinite number of modes requires distributed sensors and actuators. One method of designing a control system is to construct a truncated discrete model consisting of a limited number of modes. Sometimes this number may be very large. As a result, there are three sets of modes: modeled controlled, modeled uncontrolled (residual), and unmodeled. Let m_s be the number of modeled modes and m_c the number of controlled modes. The control system is designed to consider the modeled mode only. The active controller consists of two parts: (i) a state estimator which accepts the sensor measurements and produces an estimated state; (ii) a linear state variable feedback control based on VSC by the estimated state to produce the actuator commands U.

For control implementation, it is required to generate $\boldsymbol{U}$. This needs estimation of the modal displacements and velocities. Using a modal filter [9], one can extract modal displacements A_{mn}, B_{mn} and velocities $\dot{A}_{mn}$, $\dot{B}_{mn}$ from the measurements of the transverse displacement $W(r, \theta, t)$ and velocities $\dot{W}(r, \theta, t)$. Having the modal displacements and velocities, one can generate the modal control force. In this paper, the design of the controller is based on the independent modal space control (IMSC) method [8] which is shown in Figure 2c. The IMSC implies that the generalized controls for a certain mode depend only on that particular model. That is, each mode is controlled independently.

6. CONTROL PROCEDURE

The schematic diagram of the control implementation is given in Figure 2a and the block diagram of IVSC is shown in Figures 2b, c. These figures show that several discrete sensors are attached to the disk, and that the measured information is sent to the controller to

perform the necessary calculation. Finally, several discrete actuators are used to produce the control forces.

Estimations of A_{mn}, B_{mn} and $\dot{A}_{mn}$, $\dot{B}_{mn}$ from the outputs of sensors are generally made by either deterministic observer or modal filters. In the present work, Galerkin's discretization of the disk favors use of modal filters for this purpose. In fact this is an added advantage of the discretization procedure adopted in the analysis.

The states of the system, A_{mn}, B_{mn} and $\dot{A}_{mn}$, $\dot{B}_{mn}$, can be obtained by sensors located in the disk. The sensors provide information on actual deflections and velocities of the disk at the chosen $m_s (m_s \leqslant 2n-1)$ locations. The locations of sensors are chosen to coincide with m_s nodes of the original discretization scheme. With these m_s nodes alone forming a new discretization scheme, the deflections and velocities at the balance $(2n-1)-m_s$ nodes are interpolated.

In practical implementation, it is necessary that the number of modes is less than the order of discretization and the number of modes to be controlled is minimized. These two requirements are known to lead to observation spillover problems. While the observation spillover is due to the use of discrete sensors, the control spillover is caused by the influence of control force on controlled modes. In particular, as m_s is the number of modeled modes and m_c is the number of controlled modes, then $(2n-1)-m_s$, is the number of unmodeled modes and $m_s - m_c$ is the number of the modeled but uncontrolled modes.

The effect of the unmodeled modes always exists. However, the observation spillover is here avoided by the use of modal filters supported by proper choice in the number of sensors m_s. The selection m_s is generally dictated by the degree of participation of various modes in the disk response.

The preliminary control procedure presented above can be summarized as follows: 1. the disk vibrations are excited by the external forces or initial disturbances. 2. the measured displacements $\mathbf{X}$ and the velocities $\dot{\mathbf{X}}$ of some specific points on the disk are obtained from the output of the discrete sensors. 3. $\mathbf{X}$ and $\dot{\mathbf{X}}$ are sent to the modal filters to calculate the estimated modal co-ordinates A_{mn}, B_{mn} and their velocities $\dot{A}_{mn}$, $\dot{B}_{mn}$. 4. the output force of each discrete actuator is calculated and is applied to the disk system.

7. SIMULATION RESULTS AND DISCUSSIONS

Since the natural frequencies for all modes with one or more nodal circles are greater than the natural frequencies of modes with zero nodal circles ($n = 0$), the present analysis will include only modes with zero nodal circles and neglect higher modes. In the following simulation, the disk is modelled as a centrally clamped circular plate with elasticity modulus $E = 73\,080\ \mathrm{N/mm^2}$, mass density $\rho = 2{\cdot}8 \times 10^{-6}\ \mathrm{kg/mm^3}$, Poisson ratio $v = 0$, thickness $h = 1{\cdot}0\ \mathrm{mm}$, inner radius $a = 100\ \mathrm{mm}$, and outer radius $b = 200\ \mathrm{mm}$. The objective here is to control the low frequency vibration modes of the rotating disk. The VSC schemes proposed by Fung *et al*. [13] can make the system completely insensitive to parametric uncertainty and external disturbance.

First, the transient responses of a rotating disk with non-constant angular velocity should be investigated. The initial values are all zero except that B_{00}, A_{10} are $-0{\cdot}1$, $-0{\cdot}05$ respectively. Figure 3 shows the vibration response of the disk rotating at 700 rpm from $\tau = 0$ to $\tau = 2$ in the first step. In the second step (from $\tau = 2$ to $\tau = 4$), the disk is accelerated by a constant acceleration to 1700 rpm at $\tau = 4$. Finally, the angular velocity is held at 1700 rpm until $\tau = 6$. Conversely, the angular velocity of the disk is held at 1700 rpm in the first step, and is reduced to 700 rpm in the third step (Figure 4). A_{10} and B_{10} are coupled, so that energy can be transferred between each other. Thus the vibration amplitudes of B_{10} will be excited (Figs. 3c, 4c). One finds that the angular frequency

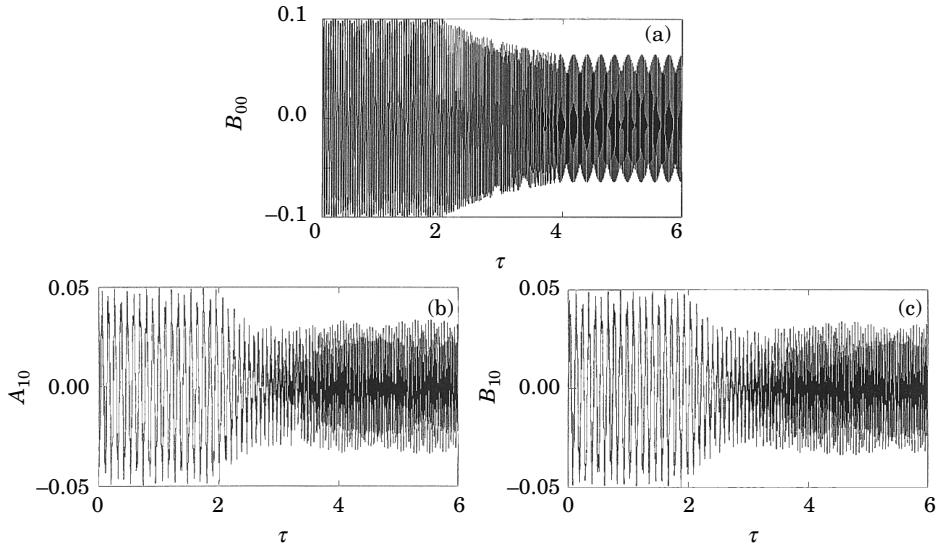

Figure 3. Transient responses of B_{00}, A_{10}, B_{10}, under different angular velocities. (a) 700 rpm, mode 1 ($0 < \tau < 2$), (b) uniformly accelerating from 700 to 1700 rpm, mode 2 ($2 < \tau < 4$), (c) 1700 rpm, mode 2 ($4 < \tau < 6$).

(1700 rpm) is very close to four times forward wave frequency and twice back wave frequency in the second mode. The quasi-periodic solution of disk vibration takes place at 1700 rpm (Figures 3b, c; 4b, c). As the rotation speed increases, the disk becomes more rigid so the amplitude decreases in the second step in Figure 3, and increases in the second step in Figure 4.

Figure 5 shows the responses of the disk with the rotating speed under different perturbation with $m_s = 3$ and $m_c = 0$. The perturbed frequency ω_f is twice the vibration

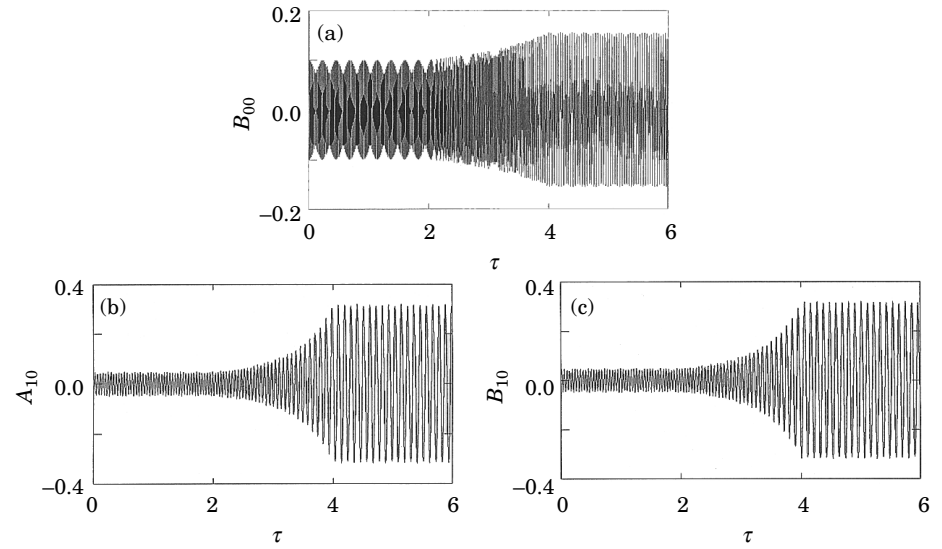

Figure 4. Transient responses of B_{00}, A_{10}, B_{10}, under different angular velocity. (a) 1700 rpm, mode 1 ($0 < \tau < 2$), (b) uniformly decelerating from 1700 to 700 rpm, mode 2 ($2 < \tau < 4$), (c) 700 rpm, mode 2 ($4 < \tau < 6$).

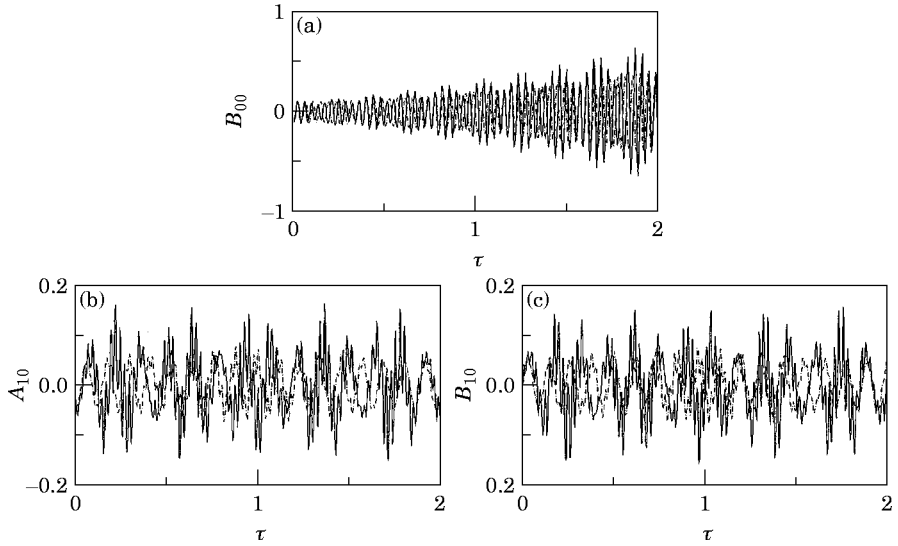

Figure 5. Transient responses of (a) B_{00} (mode 1), (b) A_{10} (mode 2), (c) B_{10} (mode 2) with angular velocity for different perturbations. $\Omega = \Omega_0 + \Omega_p \sin(\omega_f t)$, $\Omega_0 = 650$ rpm, $\omega_f = 2\omega_1$: ——, $\Omega_p = 0{\cdot}7\Omega_0$; – · –, $\Omega_p = 0{\cdot}2\Omega_0$.

frequency ω_1 of B_{00} of the rotating disk with a steady-state angular velocity ($\Omega_0 = 650$ rpm). From Figure 5a, we know the response of B_{00} is divergent. It is observed that the perturbation Ω_p is increased and the amplitude of oscillation is larger. Also, the amplitudes of the secondary mode exceeds 0·1 in Figs. 5b, c.

In this paper, the modeled mode $m_s = 3$ is used. Different controlled modes ($m_c = 2, 3$) are compared in Figure 6. From Figure 6a, mode 1 is controlled very well. In Figure 6b, the controlled mode A_{10} has slightly deteriorated transient response, because energy from high modes transfers to low modes. In Figure 6c, the transverse vibration of the uncontrolled mode of B_{10} is excited.

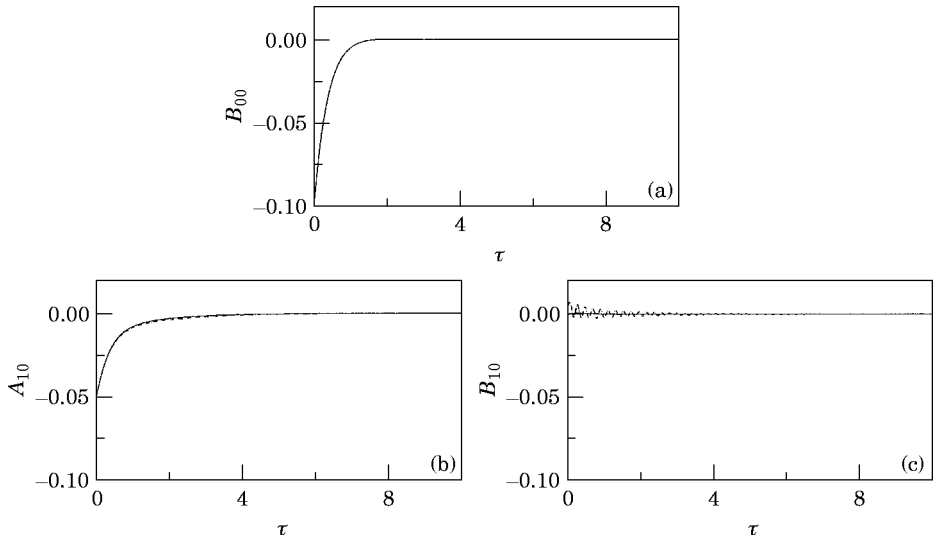

Figure 6. Controlled response with integral compensation. $m_s = 3$: – · –, $m_c = 2$; ——, $m_c = 3$. The other parameters are $K_1 = 0{\cdot}2$, $P = 0{\cdot}1$, $\alpha = 0{\cdot}5$. (a) B_{00} (mode 1); (b) A_{10} (mode 2); (c) B_{10} (mode 2).

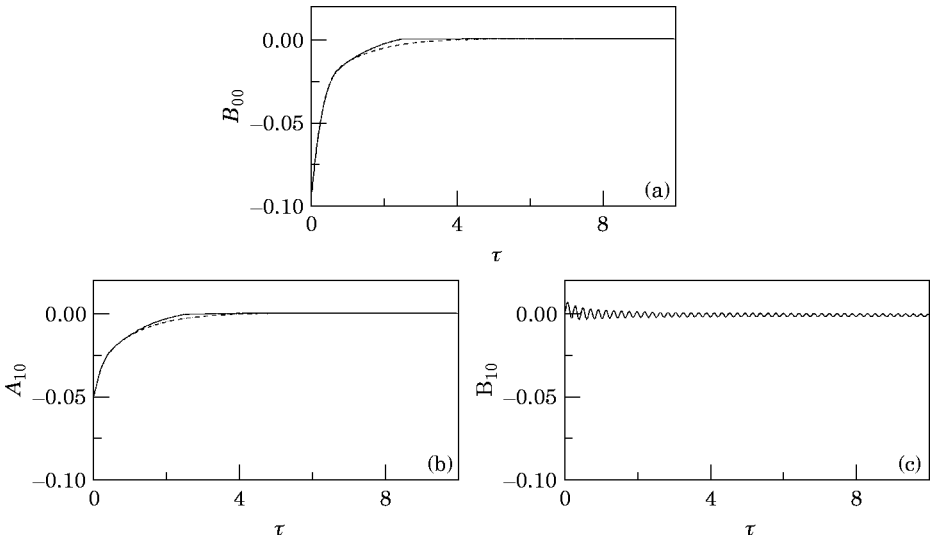

Figure 7. Comparing transient responses between IVSC (——) and VSC (– · –). The parameters are $m_s = 3$, $m_c = 2$, $K_I = 0{\cdot}2$, $P = 0{\cdot}1$, $\alpha = 0{\cdot}1$. (a) B_{00} (mode 1); (b) A_{10} (mode 2); (c) B_{10} (mode 2).

Figure 7 compares the transient responses between IVSC and VSC. The results are obviously different. The IVSC has better transient response and quickly approaches steady state especially in B_{00} and A_{10}. Since there is no control input for the B_{10} mode, the oscillations occur continuously for both IVSC and VSC schemes (Figure 7c).

In Figure 8, transient responses and steady states are compared with various power rates α. In Figure 8a, larger α produces good performance in transient responses, but the steady-state error is not guaranteed to approximate to zero in the shorter timescale. Both the transient responses and steady-state error should be considered concurrently by a trial-and-error method. From Figure 8, it is seen that $\alpha = 0{\cdot}5$ is an adequate number to minimize the oscillation of the uncontrolled mode.

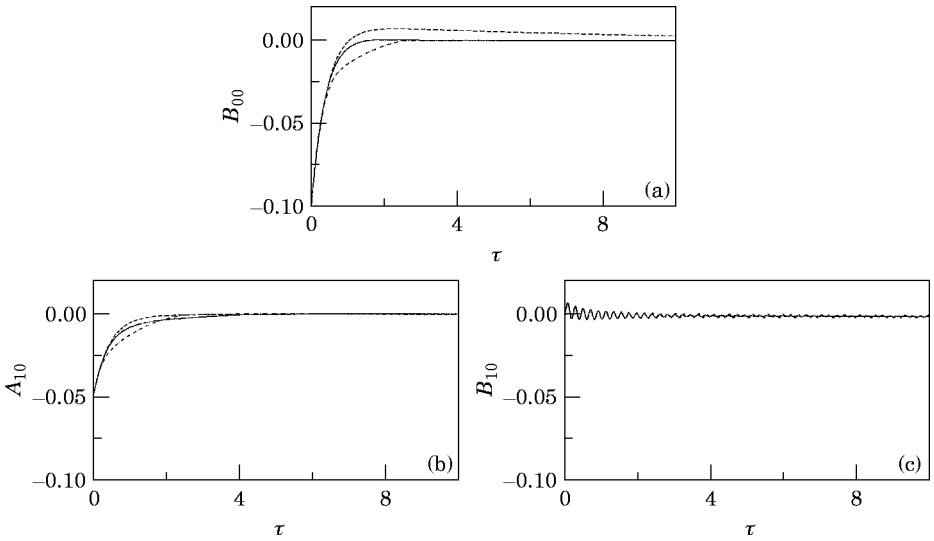

Figure 8. Controlled responses for various power rates. $m_s = 3$, $m_c = 2$: ——, $\alpha = 0{\cdot}1$; – · –, $\alpha = 0{\cdot}5$; - - -, $\alpha = 0{\cdot}9$. (a) B_{00} (mode 1); (b) A_{10} (mode 2); (c) B_{10} (mode 2).

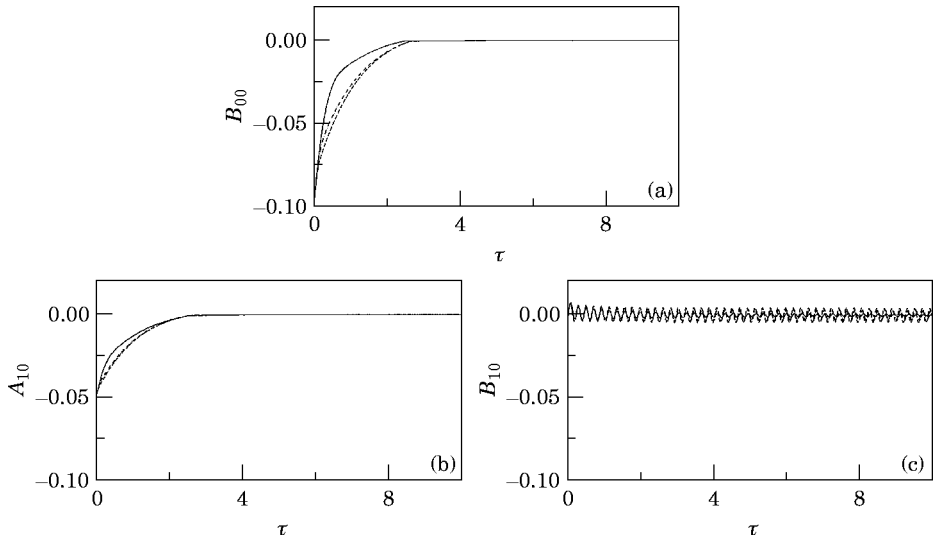

Figure 9. Controlled responses for various values of parameters P. $m_s = 3$, $m_c = 2$, $\alpha = 0{\cdot}1$: ——, $P = 0{\cdot}1$; - · - · , $P = 0{\cdot}5$; - - - , $P = 0{\cdot}9$. (a) B_{00} (mode 1); (b) A_{10} (mode 2); (c) B_{10} (mode 2).

Finally, the controlled responses are shown in Figure 9 for various values of P. One finds that as P becomes smaller the performance of the transient response is better. Also, it is obvious that steady states are similar for each P.

8. CONCLUSIONS

The governing equation of the transverse vibrations of a spinning disk system with non-constant angular velocity is obtained by Hamilton's principle. Furthermore, the partial differential equation is solved by Galerkin's method. A regulator design methodology is presented and applied to the rotating disk system by using the variable structure control with integral compensation.

The greatest advantage of this methodology is the simplicity of the solution in implementation of the control procedure, which suppresses the transverse vibration of the rotating disk with non-constant angular velocity and parameter variation. The key to this approach is the reaching law method. In the sliding mode, chattering about the switching surface is alleviated. The procedure of using this method is straightforward and easy to carry out. Numerical results show that the transverse displacement of the rotating disk quickly reaches a stable state when control forces are applied.

ACKNOWLEDGMENT

The authors are greatly indebted to the National Science Council R.O.C. for the support of the research through contract No. NSC 85-2212-E-033-006.

REFERENCES

1. H. Lamb and R. V. Southwell 1921 *Proceeding of the Royal Society*, *London* **99**, 272–280. The vibrations of a spinning disk.
2. S. Barasch and Y. Chen 1972 *ASME Journal of Applied Mechanics* 1143–1144. On the vibration of a rotating disk.

3. P. Z. Bulkeley 1973 *ASME Journal of Applied Mechanics* 133–136. Stability of transverse waves in a spinning membrane disk.
4. R. W. Ellis and C. D. Mote Jr. 1979 *ASME Journal of Dynamic System, Measurement, and Control* **101**, 44–49. A feedback vibration controller for circular saws.
5. C. J. Radcliffe and C. D. Mote Jr 1982. *ASME Journal of Dynamic System, Measurement, and Control* **105**, 39–45. Identification and control of rotation disk vibration.
6. J. N. Aubrun and M. J. Ratner 1984 *Journal of Guidance Control* **7**, 535–545. Structure control for a circular plate.
7. C. Y. Kuo and C. C. Huang 1992 *ASME Journal of Dynamic System, Measurement, and Control* **114**, 104–112. Active control of mechanical vibration in a circular disk.
8. L. Meirovitch and H. Oz 1980 *Journal of Guidance Control* **3**, 218–226. Optimal modal-space control of flexible gyroscopic system.
9. L. Meirovitch and H. Baruh 1983 *Journal of Optimization Theory and Application* **39**, 269–291. On the problem of observation spillover in self-adjoin distributed-parameter system.
10. U. Itkis 1976 *Control Systems of Variable Structure*. New York: Wiley.
11. V. I. Utkin 1978 *Sliding Modes and Their Application in Variable Structure Systems*. Moscow: Mir.
12. J. Y. Hung, W. Gao and J. C. Hung 1993 *IEEE Transactions on Industrial Electronics* **40**, 2–22. Variable structure control: a survey.
13. R. F. Fung, C. C. Liao and H. H. Huang 1995 *Transactions of the Aeronautical and Astronautic Society of the Republic of China* **27**, 191–200. Application of variable structure control in the non-constant rotating disk system.
14. R. C. Benson and D. B. Bogy 1978 *ASME Journal of Applied Mechanics* **45**, 636–642. Deflection of a very flexible spinning disk due to a stationary transverse load.
15. S. P. Timoshenko and J. N. Goodier 1974 *Theory of Elasticity* New York.
16. T. L. Chern and Y. C. Wu 1991 *IEE Proceedings-D* **138**, 439–444. Design of integral variable structure controller and application to electrohydraulic velocity servosystem.
17. W. Gao and J. C. Hung 1993 *IEEE Transactions on Industrial Electronics* **40**, 45–55. Variable structure control of non-linear systems: a new approach.

APPENDIX: NOMENCLATURE

E modulus of elasticity.
D flexural rigidity.
G modulus of elasticity in shear.
v poission's ratio.
a inner radius of disk.
b outer radius of disk.
h thickness of disk.
ρ density of disk.
w transverse displacement.
t time.
Ω angular velocity of disk.
∇ Laplacian operator.